

# Biodegradable silica nanoparticles for efficient linear DNA gene delivery

Andrés Ramos-Valle<sup>a,b</sup>, Henning Kirst<sup>a,b</sup> and Mónica L. Fanarraga<sup>a,b</sup>

<sup>a</sup>The Nanomedicine Group, Institute Valdecilla-IDIVAL, Santander, Spain; <sup>b</sup>Molecular Biology Department, Universidad de Cantabria, Santander, Spain

## ABSTRACT

Targeting, safety, scalability, and storage stability of vectors are still challenges in the field of nucleic acid delivery for gene therapy. Silica-based nanoparticles have been widely studied as gene carriers, exhibiting key features such as biocompatibility, simplistic synthesis, and enabling easy surface modifications for targeting. However, the ability of the formulation to incorporate DNA is limited, which restricts the number of DNA molecules that can be incorporated into the particle, thereby reducing gene expression. Here we use polymerase chain reaction (PCR)-generated linear DNA molecules to augment the coding sequences of gene-carrying nanoparticles, thereby maximizing nucleic acid loading and minimizing the size of these nanocarriers. This approach results in a remarkable 16-fold increase in protein expression six days post-transfection in cells transfected with particles carrying the linear DNA compared with particles bearing circular plasmid DNA. The study also showed that the use of linear DNA entrapped in DNA@SiO<sub>2</sub> resulted in a much more efficient level of gene expression compared to standard transfection reagents. The system developed in this study features simplicity, scalability, and increased transfection efficiency and gene expression over existing approaches, enabled by improved embedment capabilities for linear DNA, compared to conventional methods such as lipids or polymers, which generally show greater transfection efficiency with plasmid DNA. Therefore, this novel methodology can find applications not only in gene therapy but also in research settings for high-throughput gene expression screenings.

## ARTICLE HISTORY

Received 12 December 2023  
Revised 4 July 2024  
Accepted 23 July 2024

## KEYWORDS

Stöber method;  
silica nanoparticles;  
gene delivery;  
DNA embedment;  
gene transfection

## 1. Introduction

Gene therapy has made significant progress in recent years, leading to the approval of several groundbreaking therapies that have paved the way for the treatment of several diseases, with remarkable benefits for patients (High & Roncarolo, 1996; Cring & Sheffield, 2020). This technology includes genome editing (Yeh et al., 2019), production of therapeutic proteins in damaged areas (Doudna, 2020), or boosting the body's natural defense mechanisms against diseases (Chen et al., 2016). These approaches can be used as therapies to mitigate the impact of acquired mutations or enhance cellular functions affected by diseases. Additionally, gene transfer allows disease modeling in mice and other species, facilitating the exploration of therapeutic approaches and addressing scientific questions that are challenging to investigate in humans (Winchester, 1982). The technology has also significant potential to advance agriculture by increasing food security, reducing the need for pesticides, and improving environmental sustainability through genetic modification (Das & Sherif, 2020; Lv et al., 2020).

An effective strategy for gene transfer is to use viral vectors such as retroviruses, lentiviruses, adenoviruses, and adeno-associated viruses (Koudelka et al., 2015). Among them, lentiviral vectors are commonly used because they enable *ex vivo* cell

modification before patient reintroduction (Jackson et al., 2016). However, the use of viral vectors carries certain risks. One concern is the potential for introducing random DNA into the host genome, which can compromise the safety and efficacy of the treatment (Bock et al., 2006; Ghosh et al., 2020). Hence, several critical issues need to be addressed, including vector toxicity, non-specificity, and instability for the clinical validation of *in vivo* gene transfer methods for clinical use.

Significant advances in vector technology, particularly synthetic nucleic acid vectors, offer promising gene delivery strategies. Among these, nucleic acid-loaded nanoparticles serve as valuable tools for efficient cargo delivery, enabling gene expression (Mitchell et al., 2021), transient protein expression (Everton et al., 2021), and genome editing in target cells (Wei et al., 2020). Liposomes are among the most promising nano-vectors due to their customizability, ease of preparation, ability to accommodate genes of varying sizes, and low immunogenicity or toxicity (Buck et al., 2019; Guimarães et al., 2021). Solid-lipid nanoparticle formulations loaded with nucleic acids have also shown potential as delivery vehicles for nucleic acids in cancer treatment. However, even though lipid-based formulations have the potential to overcome different barriers, their stability remains a concern (Luo & Lu, 2023). Furthermore,

**CONTACT** Mónica L. Fanarraga  fanarrag@unican.es  Instituto de Investigación Valdecilla-IDIVAL; Universidad de Cantabria, Avda. Herrera Oria s/n, Santander, 39011, Spain

 Supplemental data for this article can be accessed online at <https://doi.org/10.1080/10717544.2024.2385376>.

© 2024 The Author(s). Published by Informa UK Limited, trading as Taylor & Francis Group.

This is an Open Access article distributed under the terms of the Creative Commons Attribution License (<http://creativecommons.org/licenses/by/4.0/>), which permits unrestricted use, distribution, and reproduction in any medium, provided the original work is properly cited. The terms on which this article has been published allow the posting of the Accepted Manuscript in a repository by the author(s) or with their consent.

transfection efficiency with linear DNA using lipid-based nano-carriers is disappointingly low. Also, compared to viruses, lipid-based nano-delivery systems are challenging to target *in vivo* because they tend to concentrate in the liver or spleen (Duan et al., 2016). Besides, they often experience a rapid release of encapsulated DNA, which results in a short burst of recombinant gene expression, which may compromise the viability of transfected cells (Puri et al., 2009). Despite varying success rates in cultured cells and preclinical research, with some gene delivery systems undergoing validation as prospective therapeutics, the development of efficient and effective gene delivery vectors continues to face challenges. Safety concerns with viral or polymer-based delivery systems remain an issue, as do the high cost and scalability barriers of complex nanoparticle synthesis (Shahryari et al., 2021).

Silica particles (SiO<sub>2</sub>) have emerged as highly valuable systems for delivering drugs and nucleic acids (Janjua et al., 2021). These nanoscale vehicles possess distinct morphologies and structures, providing numerous advantages such as large specific surface areas, adjustable particle and pore sizes, favorable mechanical and thermal stability, low toxicity, and remarkable biocompatibility (Croissant et al., 2020). Also, the properties and functionality of silica nanoparticles can be tailored by harnessing their surface chemistry (Lehman et al., 2016), which opens new avenues for their use in nanotechnology. Colloidal silica nanoparticles, in particular, have found diverse applications as additives in the production of food, cosmetics, pharmaceuticals, and other applications (Lu et al., 2010; Huang et al., 2011; Li et al., 2012; Paris & Vallet-Regí, 2020; Cox et al., 2021). As a result, the field of drug delivery has extensively explored silica nanoparticles for over six decades.

Tailoring the size, shape, and surface functionalization of silica materials has led to increased biocompatibility and efficiency of delivery. There are different methods of delivering DNA using silica nanoparticulate systems. One of them involves adsorbing DNA on the nanoparticle surface (Bharali et al., 2005; Torney et al., 2007; Kapusuz & Durucan, 2017). However, this approach may not provide sufficient protection for the DNA and limits DNA loading capacity, negatively impacting transfection and gene expression efficiencies. To address this issue, a newer design has been developed, where DNA is directly embedded within the nanoparticle itself during the synthesis process (Ramos-Valle et al., 2023). This approach offers better protection of the nucleic acids due to being included in the particles rather than being attached to the outside. This enhances their delivery efficiency, providing a protective barrier against environmental nucleases or reactive oxygen species (ROS) and enhancing the stability of the genetic cargo. Once captured by a cell, the DNA@SiO<sub>2</sub> particles dissolve intracellularly, and release the encapsulated DNA triggering adequate cell transfection rates (Ramos-Valle et al., 2023). While these silica-based nanosystems have great potential as gene delivery systems due to their targeting, safety, scalability, and storage stability, the actual volume of the silica particles limits DNA capacity and transgene expression. While it is possible to synthesize larger particles to encapsulate additional DNA molecules and potentially increase gene expression, this approach has a detrimental effect on particle uptake and transfection efficiency. Here, we enhance DNA@SiO<sub>2</sub> particle gene

expression by optimizing the process used to synthesize the particles, taking the previously published DNA@SiO<sub>2</sub> as a foundation (González-Domínguez et al., 2017; Iturrioz-Rodríguez et al., 2019; Navarro-Palomares et al., 2020; Rodríguez-Ramos et al., 2020; Ramos-Valle et al., 2023). We have focused on reducing the size of the DNA molecules to essential sequences, thereby increasing the total number of encapsulated DNA molecules. The expected outcome is the development of a simple, low-cost system that offers a promising alternative to other gene delivery systems that are less versatile and stable.

## 2. Material and methods

### 2.1. DNA production and purification

The plasmid p-DNA was produced using standard procedures in *E. coli* DH5α that had been transformed with the plasmid pH2B-EYFP (Addgene #51002, RRID:Addgene\_51002) (see below Scheme 1a). Bacteria were cultured overnight in 400 mL of Luria-Bertani (LB) broth medium supplemented with antibiotic (100 µg/ml ampicillin). Plasmid DNA was extracted and purified using a kit (PureLink™ HiPurePlasmid Maxiprep, Thermo Fisher) following the manufacturer's protocol. DNA was precipitated and resuspended in nuclease-free dH<sub>2</sub>O at 2.5 µg/ml for direct use in the particle synthesis.

Linear DNA was produced using the PCR amplification with the corresponding p-DNA as a template (Scheme 1b). The PCR mixture was composed of forward and backward-designed primers (2.5 µM, forward: 5'-GGGTCATTA GTTCATAGCCCATATATGG-3', reverse: 5'-GATTTCGGCCTATTGG TAAAAAATGAGC-3') purchased from IDT, Master Mix NZYProof 2× (1/2 of total PCR volume) containing Taq II Polymerase Enzyme, dNTPs, buffers, and plasmid DNA template (100 ng/50 µl of total volume) (Scheme 1b,c) used with a PCR program following the manufacturer's protocol.

### 2.2. Synthesis and characterization of DNA@SiO<sub>2</sub> particles

#### 2.2.1. Materials

Silica spheres containing p-DNA and l-DNA were prepared using a modified Stöber method with absolute EtOH (PanReac AppliChem, 0.79 g/ml), DNase/RNase free dH<sub>2</sub>O (Ultrapure™, Invitrogen), NH<sub>3</sub> solution (aq, 25% v/v, Suprapur®, Sigma Aldrich) and tetraethyl orthosilicate (TEOS, Sigma Aldrich, 0.933 g/ml, lot #MKCJ6565).

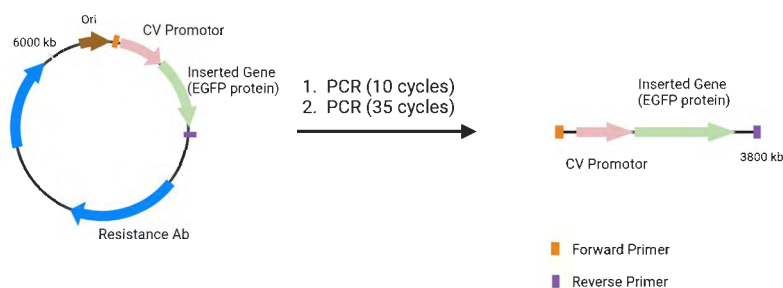
#### 2.2.2. General method for the synthesis of p-DNA@SiO<sub>2</sub> particles (p-DNA#1-6)

In a 1.5 ml microtube, the corresponding µg of purified p-DNA (see Table 1, for p-DNA#4=4.5 µg) were dispersed in 18 µl of nuclease-free ddH<sub>2</sub>O (10 M). This p-DNA solution was poured into a 1.5 ml microtube containing 59 µl of absolute EtOH. The mixture was stirred at 1,200 r.p.m for 5 min. Subsequently, 17.3 µl of ammonia 25% (1.22 M) and 5.6 µl TEOS (0.24 M) were added to this mixture (Table 1). The reaction mixture was then vortexed for 2 hours at 1,200 r.p.m. Silica spheres were centrifuged at 6,500 r.p.m, washed three times with absolute EtOH, and stored in 100 µl EtOH.

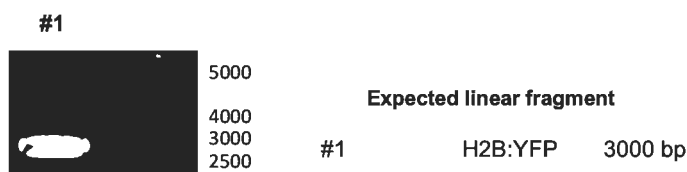
a

Plasmid	Reference and Sequence	Designed Primer 1 (Forward)	Designed Primer 2 (Reverse)
H2B: YFP	pH2B-EYFP was a gift from Rusty Lansford (Addgene plasmid # 51002 ; <a href="http://n2t.net/addgene:51002">http://n2t.net/addgene:51002</a> ; RRID:Addgene_51002)	5'- GGGTCATTAGTTCATAGCCCATAT ATGG-3'	5'- GATTCGGCCTATTGGTTAAAAA ATGAGC-3'

b



c



**Scheme 1.** p-DNA to I-DNA transformation. (a) PCR components and primer sequence design. (b) Diagram of the experimental procedure. (c) Agarose gel characterization of the synthesized I-DNA.

**Table 1.** Optimization of DNA@SiO<sub>2</sub> particle synthesis.

Entry	Synthesis				Characterization				
	NH <sub>3</sub> /M	TEOS/ M	H <sub>2</sub> O/M	Shape	DNA		Size (TEM)	Z-Size (DLS)	PDI (DLS)
					[DNA] / M (μg DNA/ mg SiO <sub>2</sub> )				
type a	1.06	0.24	3.32	plasmid	$1.4 \times 10^{-5}$ (4.5 μg)		678 ± 51	–	–
type b	1.22	0.24	9.99	plasmid	$1.4 \times 10^{-5}$ (4.5 μg)		388 ± 36	–	–
type c	0.34	0.24	14.0	plasmid	$1.4 \times 10^{-5}$ (4.5 μg)		186 ± 15	–	–
p-DNA#1	1.22	0.24	9.99	plasmid	$1.6 \times 10^{-6}$ (0.5 μg)		468 ± 28	601 ± 28	0.18 ± 0.08
p-DNA#2	1.22	0.24	9.99	plasmid	$4.8 \times 10^{-6}$ (1.5 μg)		274 ± 19	358 ± 18	0.2 ± 0.1
p-DNA#3	1.22	0.24	9.99	plasmid	$9.6 \times 10^{-6}$ (3.0 μg)		262 ± 16	324 ± 3	0.26 ± 0.02
p-DNA#4	1.22	0.24	9.99	plasmid	$1.4 \times 10^{-5}$ (4.5 μg)		393 ± 22	413 ± 67	0.23 ± 0.06
p-DNA#5	1.22	0.24	9.99	plasmid	$2.9 \times 10^{-5}$ (9 μg)		*	1874 ± 25	0.99 ± 0.05
p-DNA#6	1.22	0.24	9.99	plasmid	$4.8 \times 10^{-5}$ (15 μg)		*	3770 ± 17	1.5 ± 0.2
I-DNA#1	1.22	0.24	9.99	linear	$1.6 \times 10^{-6}$ (0.5 μg)		384 ± 40	325 ± 12	0.41 ± 0.02
I-DNA#2	1.22	0.24	9.99	linear	$4.8 \times 10^{-6}$ (1.5 μg)		311 ± 18	314 ± 28	0.35 ± 0.03
I-DNA#3	1.22	0.24	9.99	linear	$9.6 \times 10^{-6}$ (3.0 μg)		284 ± 20	236 ± 60	0.36 ± 0.06
I-DNA#4	1.22	0.24	9.99	linear	$1.4 \times 10^{-5}$ (4.5 μg)		260 ± 22	250 ± 28	0.33 ± 0.03
I-DNA#5	1.22	0.24	9.99	linear	$2.9 \times 10^{-5}$ (9 μg)		*	1034 ± 30	0.7 ± 0.3

Notes: Effect of different concentrations of the Stöber mixture (a-c). Effects of different amounts of DNA (plasmid and linear) on particle size and dispersity. Figures S1-S11 show the TEM and DLS results of characterization. Asterisk in places where (\*) TEM sizes could not be estimated due to aggregates (see Figures S5–S6, Figures S11).

TEM: transmission electron microscopy; DLS: dynamic light scattering; PDI: polydispersity index; p-DNA: plasmid DNA; I-DNA: linear DNA.

\*The concentration of the final components in the mixture considers EtOH as a solvent and is expressed in molarity (M).

### 2.2.3. General method for the synthesis of I-DNA@SiO<sub>2</sub> particles (I-DNA#1-5)

In a 1.5 ml microtube, the corresponding μg of purified I-DNA (see Table 1, for I-DNA#4 = 4.5 μg) were dispersed in 18 μl of nuclease-free ddH<sub>2</sub>O (10 M). This p-DNA solution

was poured into a 1.5 ml microtube containing 59 μl of absolute EtOH. The mixture was stirred at 1,200 r.p.m for 5 min. Subsequently, 17.3 μl of ammonia 25% (1.22 M) and 5.6 μl TEOS (0.24 M) were added to this mixture (Table 1). The reaction mixture was then vortexed for 2 hours at 1,200 r.p.m. Silica spheres were centrifuged at 6,500 r.p.m, washed three times with absolute EtOH, and stored in 100 μl EtOH.

\*The concentration of the final components in the mixture considers EtOH as a solvent and is expressed in molarity (M).

#### 2.2.4. Particle size characterization

**TEM analysis:** DNA@SiO<sub>2</sub> particles were dispersed in absolute EtOH (0.5mg/ml) and 10µl was applied to the corresponding carbon film on a copper grid for Transmission Electron Microscopy (TEM) analysis. The samples were dried for 1h at 25°C and subsequently introduced into a microscope sampler. TEM images were obtained with a JEM1011 TEM equipped with a high-resolution Gatan digital camera (JEOL, Japan). The images were then analyzed using ImageJ software ( $n=100$  particles per analysis).

**DLS analysis:** DLS size distribution measurements of p-DNA#1-6 and l-DNA#1-5 were carried out on a Malvern Ultra Zetasizer at 25°C using filtered dH<sub>2</sub>O as a dispersant. The polydispersity index (PDI) was measured following the same protocol. The measurements were repeated three times for each sample ( $n=3$ ), and the data are presented as mean±standard deviation (SD).

#### 2.3. Cell lines

HEK 293 (Human Kidney Epithelial Cells, RRID:CVCL\_0045) cells were acquired in Innoprot (Innovative Technologies in Biological Systems, Derio, Spain). HEK 293 cells were maintained in Iscove's modified Dulbecco's medium (IMDM) supplemented with 10% fetal bovine serum and gentamycin in a 5% CO<sub>2</sub> incubator at 37°C.

#### 2.4. Cell transfection assays

HEK 293 cells were seeded in a 24-well plate before transfection at a density of  $5 \times 10^4$  cells/well and incubated for 24h. After this time, DNA@SiO<sub>2</sub> particles (valid for p-DNA@SiO<sub>2</sub> and l-DNA@SiO<sub>2</sub>) washed in Phosphate Buffer Saline (PBS) and resuspended in IMDM culture medium (100µg NPs/ml) was added to each well. The medium was replaced after 16hours.

For Lipofectamine™ 2000 transfection of HEK 293 cells, 3.13µl of reagent was diluted in 496.85µl of serum-free IMDM medium and incubated for 5 minutes. 2.5µg of p-DNA was diluted in 500µl of serum-free IMDM according to the manufacturer's instructions.

At the specified time, cells were harvested, washed twice with PBS, and finally fixed in a 4% paraformaldehyde (PFA) solution for 15min before qualitative or quantitative characterization. For fluorescent microscopy, cells were stained with DAPI, washed in PBS, mounted on crystal glass coverslips, and imaged using a Nikon AIR confocal microscope. Flow cytometry was performed on fixed transfected cells at the corresponding sampling times. Approximately 10,000 cells were analyzed per sample using a CytoFLEX (Beckman Coulter) equipped with 3 excitation lasers (488nm x 50mW; 638nm x 50mW; 405nm x 80mW) and 13 fluorescence detectors. Data corresponding to the positive cell distribution were obtained with the appropriate single-cell gating. Three

different replicates were performed for each experiment ( $n=3$ ). Data are expressed as mean±standard deviation (SD).

#### 2.5. Cell cytotoxicity assays

HEK 293 cells were reseeded into 96-well culture plates at a density of  $2 \times 10^4$  cells/well and incubated for 24h. DNA@SiO<sub>2</sub> particles were washed in Phosphate Buffer Saline (PBS) and were diluted with Iscove's Modified Dulbecco's Medium (IMDM) with sera. DNA@SiO<sub>2</sub> particles were added at concentrations ranging from 0 to 400µg/ml (see Figure 3). After incubation at 37°C for 16h, the medium in each well was renewed, and the cells were incubated for 24h and 72h before the addition of 10µl of the MTT labeling reagent (Invitrogen, Cat. Number M6494, final concentration 0.5mg/ml). After incubation for 4h in a humidified atmosphere (37°C, 5–6.5% CO<sub>2</sub>), 100µl of the solubilization solution was added to each well. The plates were allowed to stand overnight in the incubator in a humidified atmosphere. The absorbance of the samples was measured using a microplate reader at 570nm.

#### 2.6. Statistical analysis

A total of 10,000 cells were analyzed per condition in three replicates of each experiment ( $n=3$ ) in Figures 1–4. Analysis *t*-tests were employed to compare the Mean Fluorescence Intensities (related bars), and 0.05 statistical analysis was used. Error bars represent SD.

### 3. Results

#### 3.1. Excess plasmid DNA results in aberrant DNA@SiO<sub>2</sub> particles

Aiming to reduce the DNA@SiO<sub>2</sub> particle size, we conducted a series of experiments, varying the stoichiometric ratios of NH<sub>3</sub>, H<sub>2</sub>O, and TEOS in the Stöber method, while maintaining consistent amounts of plasmid DNA (p-DNA) per particle. This allowed us to synthesize DNA@SiO<sub>2</sub> particles with sizes ranging from 100 to 620nm, labeled as type a-c (Table 1, Figures S2–S12). Due to the considerable size variation observed in type-c particles and their negative impact on cellular uptake, we narrowed our focus to optimize type-b particles, with a diameter of approximately 350nm.

To enhance transfection efficiency and achieve higher levels of protein expression, we proceeded to assess how the DNA content in the formulation impacts nanoparticle characteristics, such as size, morphology, and polydispersity. Our goal was to identify strategies that can optimize particle properties and maximize nucleic acid loading, thereby improving overall transfection efficiency. Proof-of-concept experiments were performed utilizing plasmid DNA (p-DNA) encoding the histone H2B tagged with yellow fluorescent protein (H2B:YFP) leading to fluorescent nuclei after transfection and protein expression. Various concentrations ranging between  $1.6 \times 10^{-6}$  M and  $4.8 \times 10^{-5}$  M of DNA were chosen to investigate the impact of nucleic acid concentration

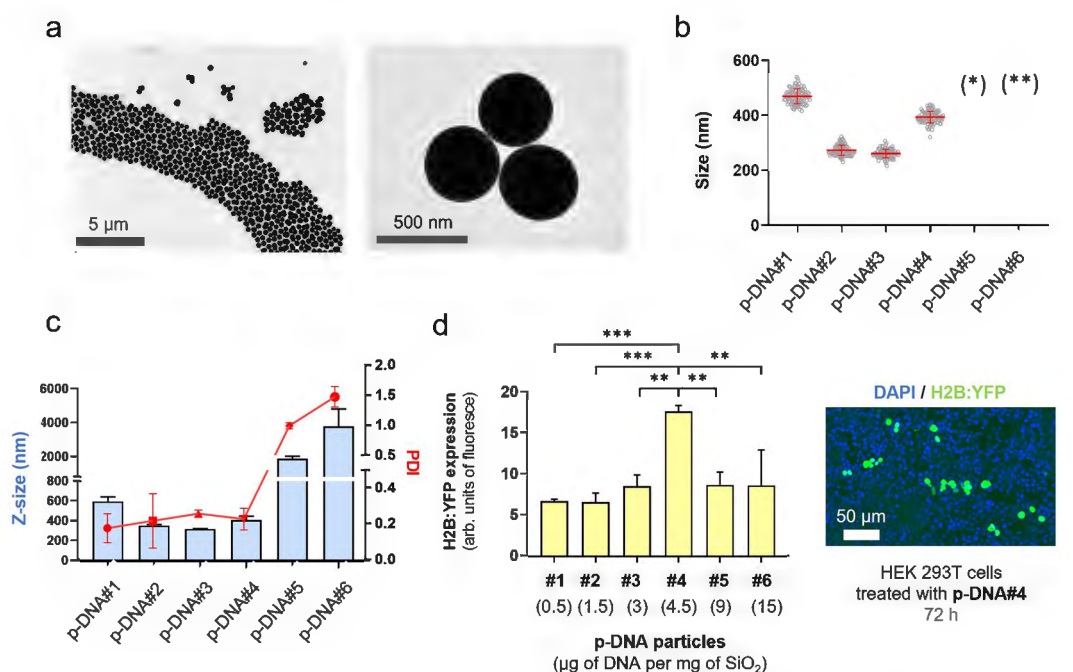


**Figure 1.** p-DNA@SiO<sub>2</sub> particles. (a) TEM images of p-DNA#4 particles with 4.5  $\mu\text{g}$  of plasmid H2B:YFP DNA. (b) Particle diameter (mean  $\pm$  SD) measured by TEM within a scatter dot plot comparing p-DNA#1-6 ( $n=100$ ). Values for p-DNA#5 and p-DNA#6 are not included due to the presence of aggregates (see Figures S8–S9). (\*)(\*\*) p-DNA#5-6 not included due to the presence of aggregates (see Figures S5–S6). (c) DLS characterization of p-DNA#1-6 bar chart of Z-size (mean  $\pm$  SD, left Y axis,  $n=3$ ) and dot plot in red showing the polydispersity index (PDI) (mean  $\pm$  SD, right Y axis,  $n=3$ ). (d) Flow cytometry quantification of the transfection efficiency (mean fluorescence intensity) of the p-DNA#4 DNA@SiO<sub>2</sub> particles and a representative confocal microscopy image of HEK 293 cells expressing the recombinant H2B:YFP protein 72 h after transfection. Data are shown as the mean  $\pm$  SD of 3 experimental replicas ( $n=10,000$  cells/replica,  $t$ -test,  $*p<0.05$ , and  $***p<0.001$ ).

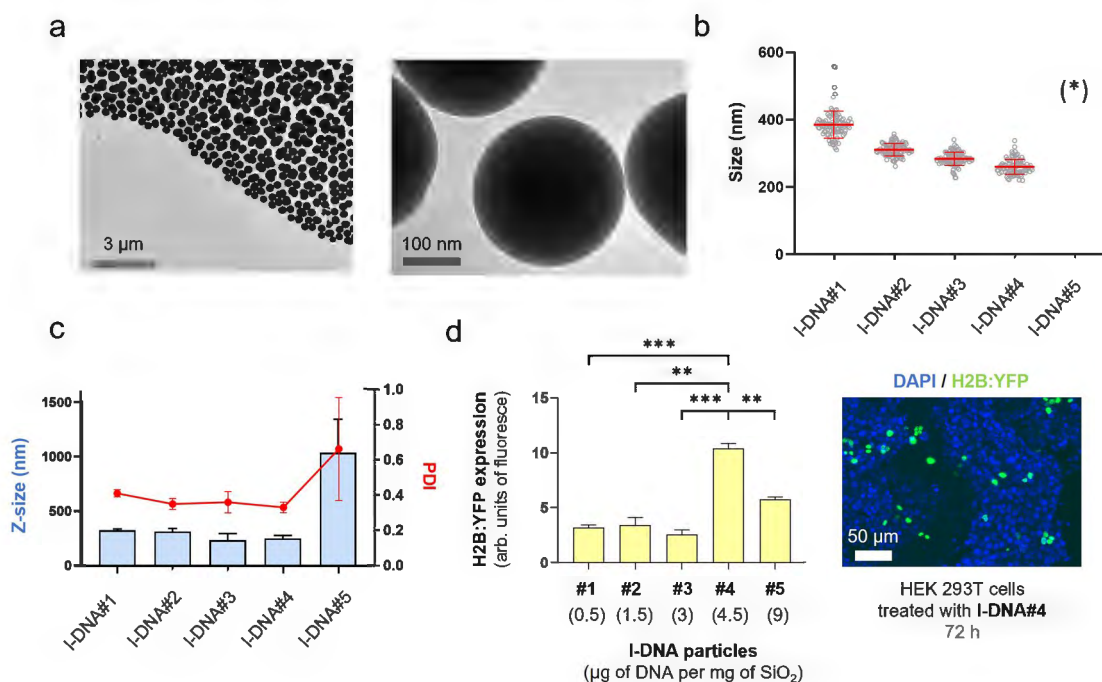


**Figure 2.** I-DNA@SiO<sub>2</sub> particles. (a) TEM images of particles I-DNA#4 with 4.5  $\mu\text{g}$  of linear H2B:YFP DNA. (b) Particle diameter (mean  $\pm$  SD) measured by TEM within a scatter dot plot comparing I-DNA#1-5 ( $n=100$ ). (\*) I-DNA#5 is not included due to the presence of aggregates (see Figure S11). (c) I-DNA#1-6 bar chart of Z-size (mean  $\pm$  SD, left Y axis,  $n=3$ ) and dot plot in red showing polydispersity index (PDI) (mean  $\pm$  SD, right Y axis,  $n=3$ ). (d) Flow cytometry quantification of the transfection efficiency (mean fluorescence intensity) of the I-DNA#4 DNA@SiO<sub>2</sub> particles and a representative confocal microscopy image of HEK 293 cells expressing the recombinant H2B:YFP protein 72 h after transfection. Data are shown as the mean  $\pm$  SD of 3 experimental replicas ( $n=10,000$  cells/replica,  $t$ -test,  $*p<0.05$ , and  $***p<0.001$ ).

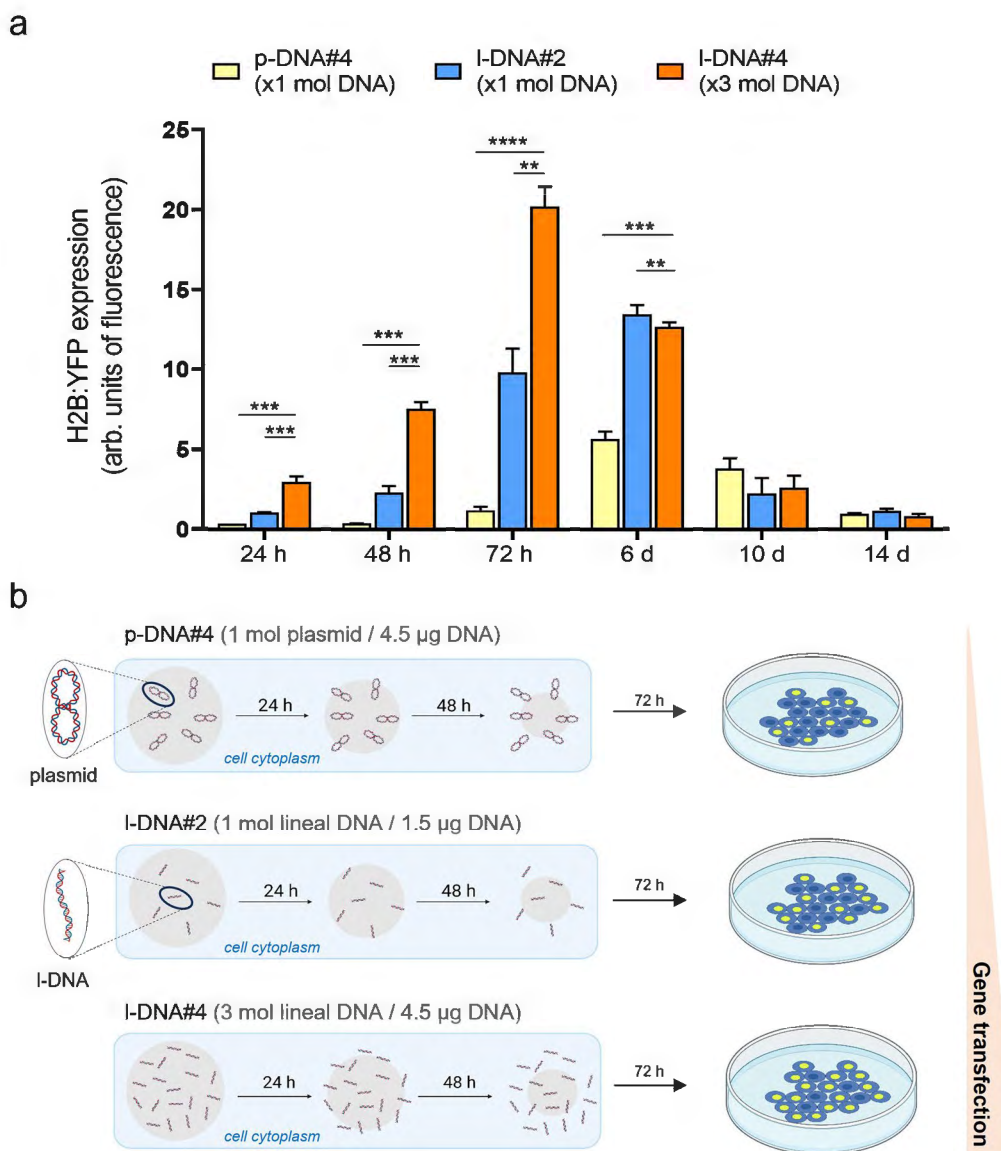


**Figure 3.** (a) Quantification of the transfection efficiency (mean fluorescence intensity) using p-DNA#4, I-DNA#2, and I-DNA#4 particles. Data are shown as the mean  $\pm$  SD of 3 experimental replicas ( $n=10,000$  cells/replica,  $t$ -test,  $**p < 0.01$ ,  $***p < 0.001$ , and  $****p < 0.0001$ ). Protein expression profile from 24 h to 14 days. (b) Mechanistic proposal of differences in gene transfection efficiency for p-DNA#4, I-DNA#2, and I-DNA#4.

on the properties of the particles. Interestingly, we observed that with an increasing amount of p-DNA per particle the particle size decreased slightly (Table 1). The sizes ranged from 600 nm for p-DNA#1 to 350 nm for p-DNA#3 (Figure 1). However, at higher DNA concentrations, there was a significant increase in particle polydispersity that was likely due to the formation of silica aggregates in p-DNA#5-6 (Figures 1(c), S5, S6). At a concentration of 4.5  $\mu$ g p-DNA per mg SiO<sub>2</sub>, the particles demonstrated the best balance of polydispersity, size, and DNA loading. This concentration yielded optimal results in terms of achieving a desirable particle size distribution and loading capacity while minimizing polydispersity.

Next, we evaluated the efficiency of various particle types on transfection using HEK 293 cells. This revealed that protein expression levels for particle types p-DNA#1-4 increased gradually and proportionally with higher amounts of p-DNA (Figure 1(d)). Our results show (Table 1, Figure 1), that a balance is required between the amount of DNA and

the concentration of the Stöber components to permit silanol polymerization and effective DNA loading while ensuring minimal polydispersity and efficient transfection of synthesized DNA@SiO<sub>2</sub> particles. The particles p-DNA#4 are the most suitable candidates because they show a well-balanced combination of maximal gene cargo loading, optimal particle morphology, and transfection efficiency (Figure 1). Furthermore, our experiments show that the total amount of DNA integrated into a silica matrix acts as a limiting factor to ensure the preservation of acceptable particle size and polydispersity index (PDI) values.

### 3.2. Linearization of plasmid DNA: influence of I-DNA size, shape and mass on DNA@SiO<sub>2</sub> particle synthesis

With this understanding, we next aimed to enhance gene delivery by increasing the coding DNA (gene copy numbers) while maintaining the total DNA mass in the formulation. To

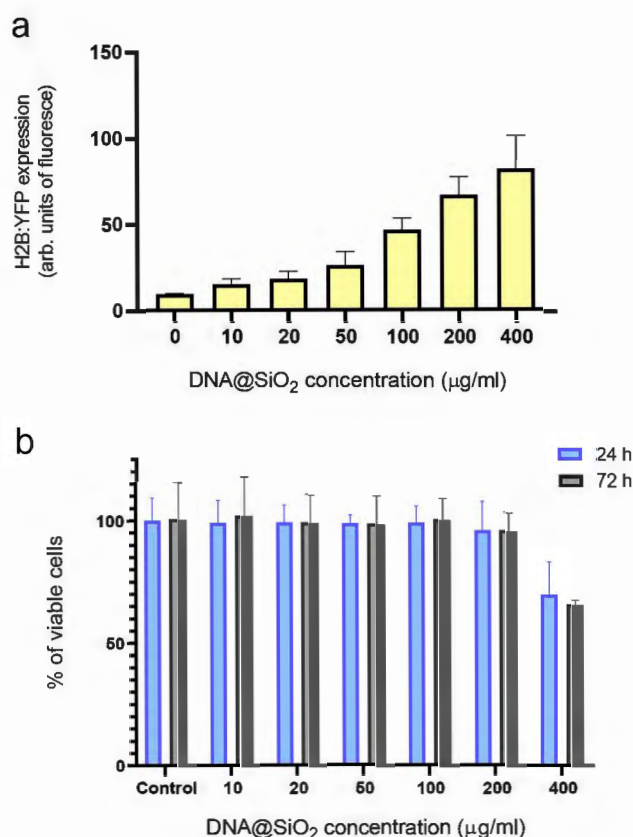


**Figure 4.** Effect of particle concentration on transfection efficiency and cell viability. (a) Flow cytometry quantification of transfected H2B:YFP protein by using I-DNA#4 particles (mean  $\pm$  SD,  $n=3$ ) carrying different DNA@SiO<sub>2</sub> concentrations ( $\mu\text{g/ml}$  IMDM). (b) MTT assay showing % of viable cells 24 h and 72 h after I-DNA#4 treatment with the same particles (mean  $\pm$  SD,  $n=6$ ).

achieve this, we used PCR with specific primers to selectively eliminate elements non-essential for the transfection of human cells, such as the origin of replication, prokaryotic selection marker, and multiple cloning sites. Through this approach, we successfully generated linear DNA (I-DNA) that exclusively contained the essential DNA sequence necessary for efficient gene expression in human cells. The synthesized I-DNA consisted of three essential elements: (i) a promoter sequence including the ribosome binding site for gene expression, (ii) the coding sequence of the gene, and (iii) a transcriptional terminator. By using I-DNA instead of p-DNA, we were able to reduce the size of the DNA molecule by approximately 60% (Scheme 1).

After obtaining the PCR products, we quantified them by UV-VIS 280 nm absorbance and confirmed their correct size through electrophoresis. To assess their functionality and ability to induce gene expression before silica encapsulation, we tested the I-DNA molecules generated by PCR through transfection into mammalian cells using Lipofectamine™ 2000. Transfections performed using conventional methods based on lipid vectors exhibited a notable reduction in efficiency compared to transfections using p-DNA consistent with previous observations (Lehner et al., 2013).

Having confirmed the functionality of the PCR-generated I-DNA molecules, we incorporated them into the synthesis reaction at different concentrations, ranging from 0.5 to 9  $\mu\text{g}$  per mg SiO<sub>2</sub> (Table 1). Similar to the observations with

p-DNA, I-DNA quantities exceeding 4.5  $\mu\text{g}$  led to particle aggregation, resulting in Z-sizes of approximately 1000 nm and a PDI of  $0.7 \pm 0.3$  (Figures 2(c), S11). Nonetheless, particles loaded with 4.5  $\mu\text{g}$  of I-DNA (I-DNA#4) demonstrated an ideal size range of 240–280 nm in diameter with a monodisperse distribution. These results indicate that, regardless of the shape and size of the DNA (p-DNA or I-DNA), the total mass of DNA in the Stöber mixture is limited to 4.5  $\mu\text{g}$  per mg SiO<sub>2</sub> to yield acceptable nanoparticle properties. Functional tests on cells showed that I-DNA@SiO<sub>2</sub> particles exhibited enhanced gene transfection efficiency compared to p-DNA@SiO<sub>2</sub> particles (Figure 2(d)), indicating that our strategy of increasing the amount of DNA molecules by encapsulating I-DNA is suitable.

### 3.3. DNA@SiO<sub>2</sub> particles improve transfection efficiency of linear DNA over plasmid DNA

The transfection efficiency of I-DNA@SiO<sub>2</sub> particles with different amounts of I-DNA was evaluated for comparison with p-DNA particles. Specifically, we prepared particles with a consistent number of DNA molecules, equivalent to 1.5  $\mu\text{g}$  DNA per mg SiO<sub>2</sub> (referred to as I-DNA#2). Furthermore, taking advantage of the capability of I-DNA to load approximately three times more DNA molecules compared to p-DNA, we encapsulated 4.5  $\mu\text{g}$  of I-DNA per mg of SiO<sub>2</sub> (referred to as I-DNA#4), ensuring that the total mass of DNA was comparable to that contained in the original p-DNA@SiO<sub>2</sub> particles (referred to as p-DNA#4).

Quantification and comparison of protein expression 72 hours after transfection using flow cytometry revealed significantly higher levels in both I-DNA#2 and I-DNA#4 particles compared to p-DNA#4 particles, with 8-fold and 16-fold increases, respectively (Figure 3(a)). On day 6 post-transfection, the expression of I-DNA was still higher than p-DNA, being twice as high as that of p-DNA, while on days 10 and 14 there were no significant differences between the two. We propose that this pattern of protein expression is due to the smaller size of the I-DNA molecules and the process of silica dissolution (Iturrioz-Rodríguez et al., 2020; Ramos-Valle et al., 2023). Because of their smaller size I-DNA molecules are surrounded by less silica than the p-DNA molecules when embedded in the particles. Assuming a constant SiO<sub>2</sub> dissolution rate in physiological conditions, I-DNA molecules would be released faster than p-DNA, because a lower amount of silica dissolution is required to free up an I-DNA molecule compared to p-DNA. This hypothesis would explain a faster expression with I-DNA#2 particles than p-DNA#4 (Figure 3(b)).

### 3.4. Effect of particle concentration on cell transfection and viability

To find the optimal concentration of I-DNA#4 particles in transfection experiments maximizing gene expression while minimizing cell damage, we incrementally increased the nanoparticle concentration in the culture. We assessed the changes in recombinant gene expression levels and also examined the cytotoxicity resulting from the presence of

these nanoparticles in the medium at both 24 and 72 hours. Gene expression quantification was performed using flow cytometry, while toxicity was evaluated through an MTT analysis. Our findings show that using I-DNA#4 particles at concentrations ranging from 100 to 200  $\mu\text{g}$  DNA/ml resulted in the most effective delivery of I-DNA, showcasing promising applications in the field of gene therapy (Figure 4).

### 3.5. DNA@SiO<sub>2</sub> particles are better suited for I-DNA compared to conventional transfection reagents

Next, we wanted to assess how the gene expression efficiency of optimized DNA@SiO<sub>2</sub> particles loaded with linear DNA (I-DNA) compares to the widely used commercially available Lipofectamine™ 2000. Thus, we transfected HEK 293 cells using both delivery systems. Lipofectamine™ 2000-transfected cells exhibited approximately three times higher gene expression when delivering plasmid DNA compared to the silica gene delivery system (Figure 5). However, the reverse was observed when linear DNA was loaded into the particles, with DNA@SiO<sub>2</sub> surpassing Lipofectamine™ 2000 transfection efficiency by approximately three-fold. More importantly, linear DNA loaded DNA@SiO<sub>2</sub> also outperformed Lipofectamine™ 2000 loaded with plasmid DNA by about 20% making it the overall superior transfection system (Figure 5).

## 4. Discussion

Transfection of non-circular DNA using conventional non-viral vectors has been limited by their reduced compactability and DNA loading capacity compared to plasmids. Our study presents a novel approach by exploring the use of innovative DNA@SiO<sub>2</sub> particles, which have already been recognized for their remarkable protection of DNA against temperature, reactive oxygen species (ROS), and nucleases, as well as their ability to sustain gene transfection for up to 14 days (Ramos-Valle et al., 2023).

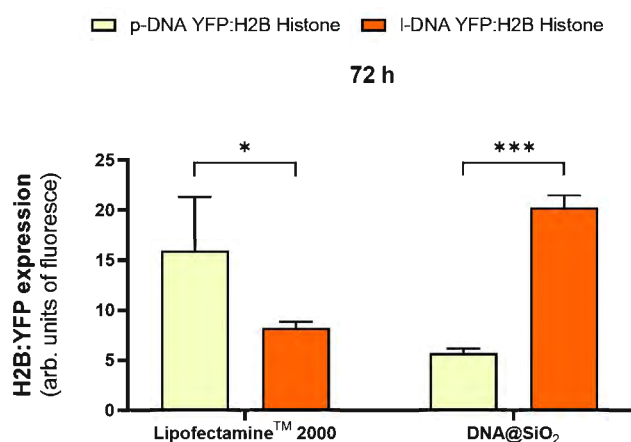


**Figure 5.** Quantification of H2B:YFP protein expression (mean fluorescence intensity) using Lipofectamine™ 2000 and DNA@SiO<sub>2</sub> system with p-DNA and I-DNA in HEK 293 cells. Data are shown as the mean  $\pm$  SD of 3 experimental replicas ( $n = 10,000$  cells/replica,  $t$ -test, \* $p < 0.05$ , and \*\*\* $p < 0.001$ ).

Unlike lipid or polymeric vectors, which typically require compact DNA morphologies for nucleic acid integration, DNA@SiO<sub>2</sub> particles can encapsulate both plasmidic and linear DNA. Since we have established a maximum loading capacity limit of 4.5  $\mu\text{g}$  DNA per mg of SiO<sub>2</sub>, we used the PCR technique to reduce the DNA molecule size to increase the copies of genes per particle. Using this approach, we could achieve a 16-fold increase in protein expression. This demonstrates the versatility of SiO<sub>2</sub> nanoparticles to encapsulate DNA regardless of its size and morphology.

When comparing the transfection efficiency of linear DNA (I-DNA) spheres with plasmid DNA (p-DNA) spheres, the protein expression peak occurred at 72 hours after transfection, thus being accelerated compared to the expression profile observed for plasmid DNA which peaked at around 6 days after transfection. We believe that the controlled release of DNA is a result of the outside-in dissolution of compact silica beads, a release mechanism that resulted in the faster release of smaller DNA fragments during transfection experiments. Additionally, linear DNA is susceptible to exonucleases and thus might have a shorter lifetime compared to plasmid DNA. In combination with the higher copy number of genes delivered this presumably leads to the observed pattern of higher and earlier peaking gene expression compared to transfection with plasmid DNA. Remarkably, I-DNA#04@SiO<sub>2</sub> particles are more efficient than standard Lipofectamine™ 2000 in I-DNA as well as p-DNA cell transfection.

While our study used linearized genes (2–4 kb), this delivery method could be adapted to deliver smaller and more diverse nucleic acids, such as oligonucleotides, which are of high interest in therapeutic applications. The results underline the potential application of this system with therapeutic oligonucleotides, as the proposed release mechanism suggests that smaller gene fragments may elicit more robust responses. In addition, the internal entrapment of the genetic cargo opens avenues for additional surface modification of nanoparticles with biomolecules to enhance nanoparticle targeting and biological properties. This would enable targeted gene transfer, avoiding potential problems and side effects associated with viral vectors. Reducing the size of nanoparticles plays a key role, as it allows for improved intercellular dispersion and thus increased cellular uptake. In addition, downsizing opens the door to adding additional layers of silica encapsulating a different gene. This would allow the time-controlled release and expression of different genes (Ramos-Valle et al., 2023). For example, this could involve inhibition of disease-related protein expression followed by activation of genes to facilitate protein repair - a promising avenue for therapeutic intervention.

## 5. Conclusion

In this study, we introduce highly efficient gene expression through a novel formulation of amorphous silica nanoparticles as a linear DNA delivery system outperforming Lipofectamine™ 2000 in cell transfection efficiency. We demonstrated that small nanoparticle size enhances intercellular and intracellular dispersion and facilitates controlled

release of plasmid and linear DNA templates. These DNA@SiO<sub>2</sub> particles show promise for gene therapy, offering superior performance in the delivery of linear DNA compared to traditional methods, and overcoming size and morphology limitations.

A key highlight of this paper is the newfound accessibility of these nanoparticles, thanks to their straightforward synthesis and composition. This quality makes them applicable across most molecular biology laboratories. What sets these particles apart is their capacity to efficiently store linear DNA, such as PCR products, and facilitate their one-step transfection or screening.

## Author contributions

Conceptualization: MLF. Methodology: ARV, HK, MLF. Validation: ARV, HK; Formal analysis: ARV, HK, MLF. Investigation: ARV, MLF. Resources: MLF; Data Curation: ARV, MLF. Writing: ARV, HK, MLF; Original Draft ARV, HK, MLF; Writing - Review & Editing ARV, HK, MLF; Supervision, MLF; Project administration: MLF. Funding acquisition: MLF.

## Disclosure statement

The author reports no conflicts of interest in this work.

## Funding

MLF acknowledges the financial support from the Spanish Instituto de Salud Carlos iii, and the European Union FEDER funds under Projects ref. PI22/00030, co-funded by the European Regional Development Fund, 'Investing in your future' and Grant TED2021-129248B-100, the Maria Zambrano Fellowship RMZ-015 funded by MCIN/AEI/10.13039/501100011033 and by the 'European Union Next Generation EU/PRTR.' We also thank the Gobierno Regional de Cantabria and IDIVAL for the project Refs IDI 20/22, INNVAL21/19, NEXTVAL 22/12, and IDI-020-022. The figures and graphs have been created with BioRender software (BioRender.com, License ID: 9519A1C8-0002).

## Data availability statement

The data presented in this study are available on request from the corresponding author.

## References

- Bharali DJ, Klejbor I, Stachowiak EK, et al. (2005). Organically modified silica nanoparticles: A nonviral vector for in vivo gene delivery and expression in the brain. *Proc Natl Acad Sci U S A* 102:11539–44. doi: [10.1073/pnas.0504926102](https://doi.org/10.1073/pnas.0504926102).
- Bock C-T, Franz S, Zentgraf H, Somerville J. (2006). Electron microscopy of biomolecules. In *Encyclopedia of molecular cell biology and molecular medicine*, 103–128. Weinheim, Germany: Wiley-VCH Verlag GmbH & Co. KGaA.
- Buck J, Grossen P, Cullis PR, et al. (2019). Lipid-based DNA therapeutics: Hallmarks of non-viral gene delivery. *ACS Nano* 13:3754–82. doi: [10.1021/acsnano.8b07858](https://doi.org/10.1021/acsnano.8b07858).
- Chen J, Guo Z, Tian H, Chen X. (2016). Production and clinical development of nanoparticles for gene delivery. *Mol Ther Methods Clin Dev* 3:16023. doi: [10.1038/mtm.2016.23](https://doi.org/10.1038/mtm.2016.23).
- Cox S, Sandall A, Smith L, et al. (2021). Food additive emulsifiers: a review of their role in foods, legislation and classifications, presence in food supply, dietary exposure, and safety assessment. *Nutr Rev* 79:726–41. doi: [10.1093/nutrit/nuaa038](https://doi.org/10.1093/nutrit/nuaa038).
- Cring MR, Sheffield VC. (2020). Gene therapy and gene correction: targets, progress, and challenges for treating human diseases. *Gene Ther* 29:3–12. doi: [10.1038/s41434-020-00197-8](https://doi.org/10.1038/s41434-020-00197-8).
- Croissant JG, Butler KS, Zink JI, Brinker CJ. (2020). Synthetic amorphous silica nanoparticles: toxicity, biomedical and environmental implications. *Nat Rev Mater* 5:886–909. doi: [10.1038/s41578-020-0230-0](https://doi.org/10.1038/s41578-020-0230-0).
- Das PR, Sherif SM. (2020). Application of exogenous dsRNAs-induced RNAi in agriculture: challenges and triumphs. *Front Plant Sci* 11:946. doi: [10.3389/fpls.2020.00946](https://doi.org/10.3389/fpls.2020.00946).
- Doudna JA. (2020). The promise and challenge of therapeutic genome editing. *Nature* 578:229–236. doi: [10.1038/s41586-020-1978-5](https://doi.org/10.1038/s41586-020-1978-5).
- Duan L, Yan Y, Liu J, et al. (2016). Target delivery of small interfering RNAs with vitamin E-coupled nanoparticles for treating hepatitis C. *Sci Rep* 6:24867. doi: [10.1038/srep24867](https://doi.org/10.1038/srep24867).
- Everton E, Rizvi F, Smith AR, et al. (2021). Transient yet robust expression of proteins in the mouse liver via intravenous injection of lipid nanoparticle-encapsulated nucleoside-modified mRNA. *Bio Protoc* 11:e4184. doi: [10.21769/BioProtoc.4184](https://doi.org/10.21769/BioProtoc.4184).
- Ghosh S, Brown AM, Jenkins C, Campbell K. (2020). Viral vector systems for gene therapy: a comprehensive literature review of progress and biosafety challenges. *Appl Biosaf* 25:7–18. doi: [10.1177/1535676019899502](https://doi.org/10.1177/1535676019899502).
- González-Domínguez E, Iturrioz-Rodríguez N, Padín-González E, et al. (2017). Carbon nanotubes gathered onto silica particles lose their biomimetic properties with the cytoskeleton becoming biocompatible. *Int J Nanomedicine* 12:6317–28. doi: [10.2147/IJN.S141794](https://doi.org/10.2147/IJN.S141794).
- Guimarães D, Cavaco-Paulo A, Nogueira E. (2021). Design of liposomes as drug delivery system for therapeutic applications. *Int J Pharm* 601:120571. doi: [10.1016/j.ijpharm.2021.120571](https://doi.org/10.1016/j.ijpharm.2021.120571).
- High KA, Roncarolo MG. (1996). Gene therapy. *Scientist* 10:455–64.
- Huang X, Li L, Liu T, et al. (2011). The shape effect of mesoporous silica nanoparticles on biodistribution, clearance, and biocompatibility in vivo. *ACS Nano* 5:5390–9. doi: [10.1021/nn200365a](https://doi.org/10.1021/nn200365a).
- Iturrioz-Rodríguez N, Correa-Duarte M, Fanarraga ML. (2019). Mesoporous silica particles as controlled drug delivery systems in cancer. *Int J Nanomedicine* 14:3389–401. doi: [10.2147/IJN.S198848](https://doi.org/10.2147/IJN.S198848).
- Iturrioz-Rodríguez N, Correa-Duarte MA, Valiente R, Fanarraga ML. (2020). Engineering sub-cellular targeting strategies to enhance safe cytosolic silica particle dissolution in cells. *Pharmaceutics* 12:487. doi: [10.3390/pharmaceutics12060487](https://doi.org/10.3390/pharmaceutics12060487).
- Jackson HJ, Rafiq S, Brentjens RJ. (2016). Driving CAR T-cells forward. *Nat Rev Clin Oncol* 13:370–83. doi: [10.1038/nrclinonc.2016.36](https://doi.org/10.1038/nrclinonc.2016.36).
- Janjua TI, Cao Y, Yu C, Popat A. (2021). Clinical translation of silica nanoparticles. *Nat Rev Mater* 6:1072–4. doi: [10.1038/s41578-021-00385-x](https://doi.org/10.1038/s41578-021-00385-x).
- Kapusuz D, Durucan C. (2017). Exploring encapsulation mechanism of DNA and mononucleotides in sol-gel derived silica. *J Biomater Appl* 32:114–25. doi: [10.1177/0885328217713104](https://doi.org/10.1177/0885328217713104).
- Koudelka KJ, Pitek AS, Manchester M, Steinmetz NF. (2015). Virus-based nanoparticles as versatile nanomachines. *Annu Rev Virol* 2:379–401. doi: [10.1146/annurev-virology-100114-055141](https://doi.org/10.1146/annurev-virology-100114-055141).
- Lehman SE, Mudunkotuwa IA, Grassian VH, Larsen SC. (2016). Nano-bio interactions of porous and nonporous silica nanoparticles of varied surface chemistry: a structural, kinetic, and thermodynamic study of protein adsorption from rpmi culture medium. *Langmuir* 32:731–42. doi: [10.1021/acs.langmuir.5b03997](https://doi.org/10.1021/acs.langmuir.5b03997).
- Lehner R, Wang X, Hunziker P. (2013). Plasmid linearization changes shape and efficiency of transfection complexes. *Eur J Nanomed* 5:205–12.
- Li Z, Barnes JC, Bosoy A, et al. (2012). Mesoporous silica nanoparticles in biomedical applications. *Chem Soc Rev* 41:2590–605. doi: [10.1039/c1cs15246g](https://doi.org/10.1039/c1cs15246g).
- Lu J, Liang M, Li Z, et al. (2010). Efficiency of mesoporous silica nanoparticles for cancer therapy in animals. *Small* 6:1794–805. doi: [10.1002/smll.201000538](https://doi.org/10.1002/smll.201000538).
- Luo WC, Lu X. (2023). Solid lipid nanoparticles for drug delivery. *Methods Mol Biol* 2622:139–46. doi: [10.1007/978-1-0716-2954-3\\_12](https://doi.org/10.1007/978-1-0716-2954-3_12).

- Lv Z, Jiang R, Chen J, Chen W. (2020). Nanoparticle-mediated gene trans-formation strategies for plant genetic engineering. *Plant J* 104:880–91. doi: [10.1111/tpj.14973](https://doi.org/10.1111/tpj.14973).
- Mitchell MJ, Billingsley MM, Haley RM, et al. (2021). Engineering precision nanoparticles for drug delivery. *Nat Rev Drug Discov* 20:101–24. doi: [10.1038/s41573-020-0090-8](https://doi.org/10.1038/s41573-020-0090-8).
- Navarro-Palomares E, González-Saiz P, Renero-Lecuna C, et al. (2020). Dye-doped biodegradable nanoparticle SiO<sub>2</sub> coating in zinc- and iron-oxide nanoparticles to improve biocompatibility and in vivo imaging studies. *Nanoscale* 12:6164–75. doi: [10.1039/c9nr08743e](https://doi.org/10.1039/c9nr08743e).
- Paris JL, Valler-Regi M. (2020). Mesoporous silica nanoparticles for co-delivery of drugs and nucleic acids in oncology: A review. *Pharmaceutics* 12:526. doi: [10.3390/pharmaceutics12060526](https://doi.org/10.3390/pharmaceutics12060526).
- Puri A, Loomis K, Smith B, et al. (2009). Lipid-based nanoparticles as pharmaceutical drug carriers: from concepts to clinic. *Crit Rev Ther Drug Carrier Syst* 26:523–80. doi: [10.1615/critrevtherdrugcarriersyst.v26.i6.10](https://doi.org/10.1615/critrevtherdrugcarriersyst.v26.i6.10).
- Ramos-Valle A, Marín-Caba L, Hevia LG, et al. (2023). One-pot synthesis of compact DNA silica particles for gene delivery and extraordinary DNA preservation. *Mater. Today Adv* 18:100357. doi: [10.1016/j.mtadv.2023.100357](https://doi.org/10.1016/j.mtadv.2023.100357).
- Rodríguez-Ramos A, Marín-Caba L, Iturriz-Rodríguez N, et al. (2020). Design of polymeric and biocompatible delivery systems by dissolving mesoporous silica templates. *Int J Mol Sci* 21:1–15.
- Shahyari A, Burtcher I, Nazari Z, Lickert H. (2021). Engineering gene therapy: advances and barriers. *Adv Ther* 4:2100040.
- Torney F, Trewyn BG, Lin VSY, Wang K. (2007). Mesoporous silica nanoparticles deliver DNA and chemicals into plants. *Nat Nanotechnol* 2:295–300. 2007 25 doi: [10.1038/nnano.2007.108](https://doi.org/10.1038/nnano.2007.108).
- Wei T, Cheng Q, Min YL, et al. (2020). Systemic nanoparticle delivery of CRISPR-Cas9 ribonucleoproteins for effective tissue specific genome editing. *Nat Commun* 11:3232. doi: [10.1038/s41467-020-17029-3](https://doi.org/10.1038/s41467-020-17029-3).
- Winchester B. (1982). Animal models of human genetic diseases. *Trends Biochem. Sci* 7:71–4. doi: [10.1016/0968-0004\(82\)90081-0](https://doi.org/10.1016/0968-0004(82)90081-0).
- Yeh CD, Richardson CD, Corn JE. (2019). Advances in genome editing through control of DNA repair pathways. *Nat Cell Biol* 21:1468–78. doi: [10.1038/s41556-019-0425-z](https://doi.org/10.1038/s41556-019-0425-z).